

Original Article

Histological Characteristics of the Regression of Corpora Lutea in Wistar Hannover Rats: the Comparisons with Sprague-Dawley Rats

Junko Sato^{1*}, Satomi Hashimoto¹, Takuya Doi¹, Naoaki Yamada¹, and Minoru Tsuchitani¹

¹ Pathology Department, Kashima Laboratory, Nonclinical Research Center, LSI Medience Corporation, 14-1 Sunayama, Kamisu, Ibaraki 314-0255, Japan

Abstract: We examined the ovaries of 44 Wistar Hannover (RccHanTM:WIST) (WH) and 30 Sprague-Dawley (SD) rats at 32-weeks of age to determine whether the ovarian structure and formation/regression of the corpora lutea (CLs) differ between the two strains. The average ovary weight was higher in WH rats. The average number of all CLs, including currently formed and previously formed CLs, was higher in WH rats in all cycles; however, no appreciable difference was detected in the number of newly or currently formed CLs between the two strains. CLs regression characterized by degeneration and necrosis of luteal cells began to appear in diestrus in both strains; however, the distribution of degenerated/necrotic cells in CLs differed. Necrotic cells were scattered in SD rats but were focally observed in the center of the CL in WH rats. The reduction in size of previously formed CLs accompanied by regression started about 2 or more stages later in WH rats than in those of SD rats. In conclusion, the higher number of CLs in WH rats is considered to be due to slow CL regression compared with in SD rats. (DOI: 10.1293/tox.2013-0054; J Toxicol Pathol 2014; 27: 107–113)

Key words: Wistar Hannover, Sprague-Dawley, rat, ovary, corpora lutea, estrous cycle

Introduction

Follicular development, atresia, luteal formation and regression recur in the ovaries, and the characteristics of the ovaries, including the follicles and corpora lutea (CLs), are specific for each estrous cycle. CLs are classified as follows: newly formed CLs, which are formed soon after ovulation; currently formed CLs, which are new CLs that form within one cycle after ovulation; and previously formed CLs, which are CLs present after one estrous cycle until their complete dissolution in the ovarian parenchyma^{1–3}. Because multiple types of CL exist in the rat ovarian parenchyma, they can be detected in one ovarian section. Thus, normal rat ovaries have regressing and residual CL features as well as specific features that represent stages of the estrous cycle. Although specific features of the estrous cycle have been well investigated, there are few reports describing luteal regression during several cycles^{4, 5}.

In recent years, Wistar Hannover (WH) rats have become increasingly commonly used for toxicological stud-

ies in Japan, and several studies on their suitability for this purpose have been published^{6–8}. In our own studies to collect background data for a subchronic (26-week) general toxicity study, we found that the pattern of CL regression differed between WH and Sprague-Dawley (SD [CrI:CD]) (SD) rats. Necrotic cells were scattered in SD rats but focally observed in the center of the CL in WH rats during luteal regression. Liberati *et al.* also reported that the percentage of pregnancies and litter size of WH rats (Tac: Glx: WifBR) were lower compared with SD rats⁹. Further, the ovaries of WH rats (at 19 and 32 weeks of age) are approximately 1.5 times heavier than those of SD rats⁶. If histological differences exist between the normal ovaries of WH and SD rats, they must be characterized in detail to evaluate toxicological data acquired using each strain. Here, in order to reveal the features of CL regression, we examined differences in the number of CLs, their size and temporal changes in morphology between WH and SD rats.

Materials and Methods

Animals

Forty-four WH (RccHanTM:WIST) female rats from Japan Laboratory Animals, Inc. (Saitama, Japan), and 30 SD (CrI:CD) female rats from Charles River Laboratories Japan (Yokohama, Japan) were individually housed in hanging-type stainless steel wire mesh cages (195 mm [w] × 325 mm [d] × 180 mm [h]; Tokiwa Kagaku Kikai Co., Ltd., Tokyo, Japan) in an animal room maintained at 22 ± 3 °C, with a

Received: 18 September 2013, Accepted: 6 January 2014

Published online in J-STAGE: 24 February 2014

*Corresponding author: J Sato (e-mail: Satou.Junko@ms.medience.co.jp)

©2014 The Japanese Society of Toxicologic Pathology

This is an open-access article distributed under the terms of the Creative Commons Attribution Non-Commercial No Derivatives (by-nc-nd) License <<http://creativecommons.org/licenses/by-nc-nd/3.0/>>.

relative humidity of $50\% \pm 20\%$, 6–20 air changes/h and a 12-h light/dark cycle. A diet of pelleted food (radiation sterilized CR-LPF; Oriental Yeast Co., Ltd., Tokyo, Japan) and tap water supplied automatically were provided *ad libitum*. The animals were cared for in accordance with the principles outlined in the guides for the care and use of laboratory animals prepared by the Japanese Association for Laboratory Animal Science and our institution.

Histology

Animals at 32 weeks of age were anesthetized using an intraperitoneal injection of sodium thiopental and then euthanized by exsanguination from the abdominal aorta to collect background data for a subchronic (26-week) general toxicity study. The ovaries, uterus, vagina and other organs/tissues were excised, weighed, fixed in 10% phosphate-buffered formalin solution, and embedded in paraffin. The paraffin blocks were serially sectioned into 4- μ m slices transverse to the plane of the ovaries. The sections were stained with hematoxylin and eosin (HE). Ovarian sections with a normal estrous cycle were chosen according to a microscopic examination of the ovaries, uterus and vagina, and the ovaries of 42 WH and 30 SD were selected. The ovarian sections were subjected to immunohistochemical analysis using an anti-Iba-1 antibody (polyclonal rabbit anti-Iba1; 1:1000, Wako, Osaka, Japan). Immune complexes were detected using a labeled streptavidin biotin (LSAB) kit (DAKO Japan Co., Ltd., Kyoto, Japan). Apoptotic cells were identified using a commercial TUNEL method (ApopTag® Peroxidase In Situ Apoptosis Detection Kit; EMD Millipore Corporation, Billerica, MA, USA).

The estrous cycle was determined by microscopic examination of the ovaries, uterine horn and vagina according to the criteria of previous reports^{1–3}. CLs were categorized as either currently (including newly formed CLs) or previously formed CLs based on the criteria described previously¹. Currently formed CLs refers to the most recently formed or new CLs observed within the first estrous cycle after ovulation. Previously formed CLs refer to the remaining CLs observed throughout several estrous cycles before their complete dissolution.

The number of CLs in HE sections was counted visually in the transverse plane of the bilateral ovaries, and categorized as described above.

Image analysis

We compared the ovarian size of the transverse plane of the bilateral ovaries in HE-stained sections between WH and SD rats using image analysis software (Image-Pro Plus; Media Cybernetics Inc., Rockville, MD, USA).

Statistical analysis

The data concerning the number of CLs and ovarian size for the two strains were tested by the F test for homogeneity of variance. When the variances were homogeneous, the t-test was used, and when the variances were heterogeneous, the Aspin-Welch test was performed (Microsoft Office Excel 2003; Microsoft Corporation, Redmond, WA, USA).

Results

Organ weight

The average weights of the WH and SD rat ovaries were 97.3 mg and 82.3 mg, respectively. The ovaries of WH rats were approximately 1.2 times heavier than those of SD rats.

Number of CLs

The average numbers of currently and previously formed CLs in one ovarian section in each estrous cycle are shown in Table 1. The average number of currently formed CLs did not significantly differ between the two strains; however, the average number of previously formed CLs in each estrous cycle of WH rats ranged from 1.3 to 2.1 times higher than those of SD rats.

Image analysis

Table 2 shows that the average sizes of the bilateral ovaries per section in each estrous cycle of WH and SD rats were comparable with the exception of their smaller size during diestrus in SD rats.

Histology

First cycle after ovulation: No marked differences were noted in estrus or metestrus between WH and SD rats in currently formed CLs, including newly formed CLs at the first cycle after ovulation (Fig. 1A–D and 1E–H). Newly formed CLs in estrus were characterized by small and spindle-shaped luteal cells with basophilic cytoplasm with or

Table 1. Average Number of CLs per Section

Strain	WH		SD	
	Currently formed CLs	Previously formed CLs	Currently formed CLs	Previously formed CLs
Estrous cycle				
Estrus	3.1 \pm 1.5	27.1 \pm 6.6**	3.0 \pm 1.6	15.9 \pm 2.0
Metestrus	3.6 \pm 1.7†	31.4 \pm 6.5##	5.4 \pm 2.4	14.8 \pm 5.3
Diestrus	4.9 \pm 2.3	22.0 \pm 7.9#	4.3 \pm 1.3	11.3 \pm 5.2
Proestrus	4.7 \pm 2.3	22.6 \pm 8.0	5.6 \pm 3.6	16.9 \pm 6.5
Average \pm standard deviation	4.2 \pm 2.1	25.2 \pm 8.1	4.6 \pm 2.6	15.1 \pm 5.0

Significant difference from SD rats (one-sided t-test): † $p < 0.05$. Significant difference from SD rats (two-sided t-test): # $p < 0.05$; ## $p < 0.01$. Significant difference from SD rats (two-sided Welch's test): ** $p < 0.01$.

without a cavity remaining in the center of the CL. Luteal cells in currently formed CLs in metestrus were larger and contained less basophilic cytoplasm compared with those present during estrus.

The currently formed CLs became large, and these luteal cells began to degenerate at diestrus in both strains; however, the distribution of the degenerated cells was different between strains. For example, there was massive or insular degeneration near the center of the CL in WH rats (Fig. 1I and 1J), while scattered single-cell degeneration was evident in SD rats (Fig. 1K and 1L) in currently formed CLs.

In proestrus, massive degeneration of luteal cells pro-

gressed to massive coagulative necrosis in the center of currently formed CLs in WH rats, degenerating cells with large vacuoles were present, and foamy macrophages surrounded the necrotic area (Fig. 1M and 1N). In contrast, single-cell necrosis of pyknotic luteal cells was scattered in currently formed CLs in SD rats (Fig. 1O and 1P). These necrotic cells were positive by the TUNEL method. Massive necrosis or fibrosis in the center of currently formed CLs was also occasionally present in SD rats; however, the incidence was much lower than that of WH rats. During the first cycle after ovulation, CL sizes were equivalent in each estrous cycle between WH and SD rats.

Second cycle after ovulation: The designation of CL changes from currently formed CLs to previously formed CLs in the second cycle of estrous after ovulation. Although previously formed CLs of SD rats began to decrease in size gradually during CL regression (Fig. 2C, 2G, 2K and 2O), those of WH rats decreased in size more slowly (Fig. 2A, 2E, 2I and 2M). In estrus, a massive necrotic area surrounded by macrophages remained in the center of previously formed CLs in WH rats (Fig. 2A and 2B), while contrast, previously formed CLs began to contain a fibrotic area in

Table 2. Average Size of Ovaries

Strain Estrous cycle	WH		SD	
	Size (mm ²)	n	Size (mm ²)	n
Estrus	15.252 ± 3.33	9	16.997 ± 2.42	9
Metestrus	15.643 ± 3.29	9	14.463 ± 1.50	10
Diestrus	15.150 ± 2.66 [#]	8	12.764 ± 0.84	4
Proestrus	14.341 ± 2.15	18	15.956 ± 2.73	7

Significant difference from SD rats (one-sided t-test). [#] p<0.05.

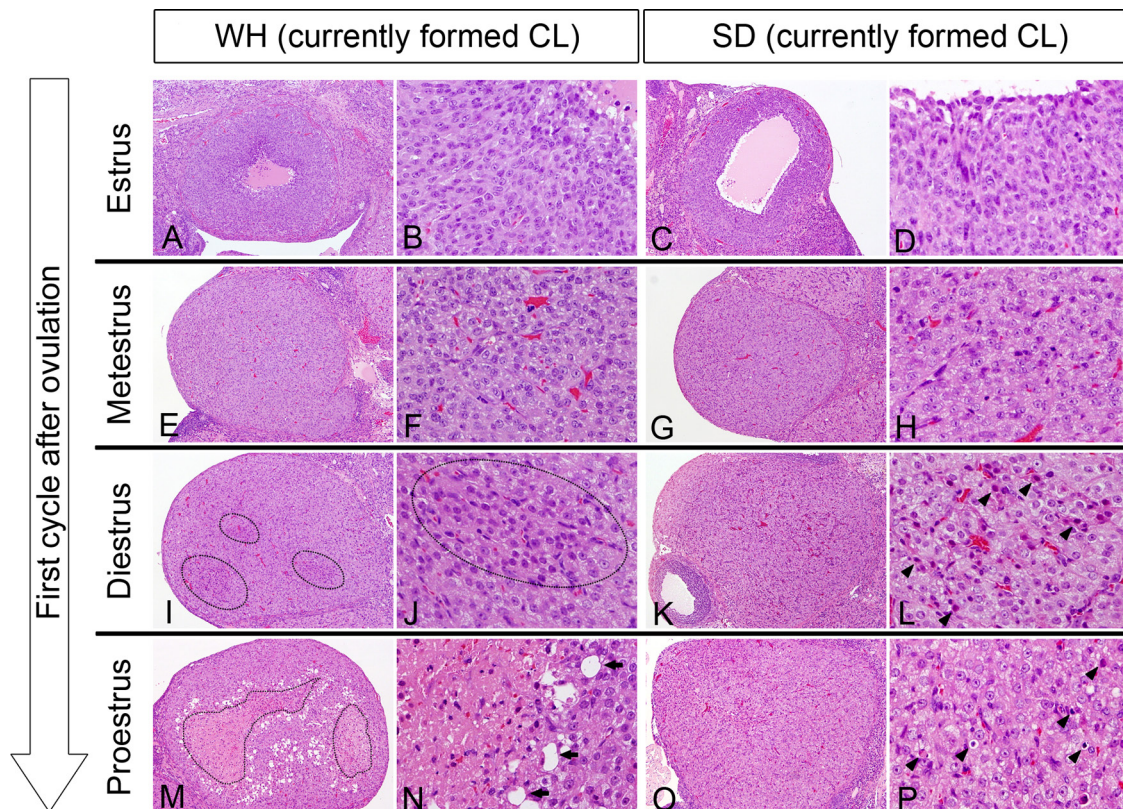


Fig. 1. Currently formed CLs in each estrous cycle at the first cycle after ovulation of WH rats and SD rats. No marked differences were noted in estrus or metestrus between WH (A, B, E, F) and SD (C, D, G, H) rats. Currently formed CLs in diestrus showed large sizes in WH (I) and SD (K) rats. There was a massive distribution of the degenerated or necrotic luteal cells in WH rats (I, J, M, N, circles) and a scattered distribution in SD rats (K, L, O, P) in diestrus and proestrus. Massive coagulative necrosis in the center of the CL in WH rats (N). Arrows show degenerating luteal cells with large vacuoles in WH rats, and arrowheads show single-cell necrosis/degeneration in SD rats. HE staining. A, C, E, G, I, K, M, O; ×40. B, D, F, H, J, L, N, P; ×300.

SD rats (Fig. 2D).

After estrus, the necrotic area of previously formed CLs was replaced by foamy macrophages in WH rats (Fig. 2E, 2F, 2I, 2J, 2M and 2N). In SD rats, the fibrotic area increased gradually, and interstitial cells (vascular endothelial cells and fibroblasts) became prominent (Fig. 2G, 2H, 2K, 2L, 2O and 2P).

The sizes of the currently formed CLs were almost comparable in both strains (Fig. 3). In contrast, previously formed CLs in SD rats were smaller than those in WH rats. In each estrous stage, the sizes of previously formed CLs of SD rats were obviously smaller than those of currently formed CLs (Fig. 3B); however, the sizes of previously formed CLs of WH rats in diestrus and proestrus were equivalent to or a little smaller than currently formed CLs (Fig. 3A and 3C), and in estrus, previously formed CL sizes were smaller than those of currently formed CLs (Fig. 3E and 3F). These results suggested that the size of the CL in WH rats decreased 2 or more stage later than in SD rats.

Macrophage infiltration

In metestrus of the first cycle after ovulation, currently formed CLs contained some macrophages that were stained by an anti-Iba-1 antibody in WH (Fig. 4A) and SD rats (Fig.

4B). In diestrus, the Iba-1-positive macrophages in currently formed CLs were more apparent in both strains than those in metestrus (Fig. 4C and 4D). In proestrus of the first cycle and in estrus of the second cycle after ovulation, macrophages either accumulated around necrotic areas or were scattered widely in the CLs in WH rats (Fig. 4E and 4G), and SD rats (Fig. 4F and 4H), respectively. This pattern was also observed during metestrus of the second cycle after ovulation in SD rats (Fig. 4I), but in WH rats, macrophages began to accumulate and replace the necrotic area (Fig. 4I).

Discussion

A summary of CL regression is shown in Table 3. Regression started in the currently formed CLs in diestrus of the first cycle after ovulation and was similar in both strains; however, the size of the CL in WH rats decreased 2 or more stages later. This time lag is related to the different pattern of luteal cell apoptosis/necrosis. Luteal cell apoptosis and phagocytosis by macrophages in SD rats cause a rapid decrease in CL size. In contrast, this process is slower in WH rats because more time is required to resorb the large mass of coagulative necrosis formed in the centers of CLs. We also demonstrated here that the ovaries of WH rats were ap-

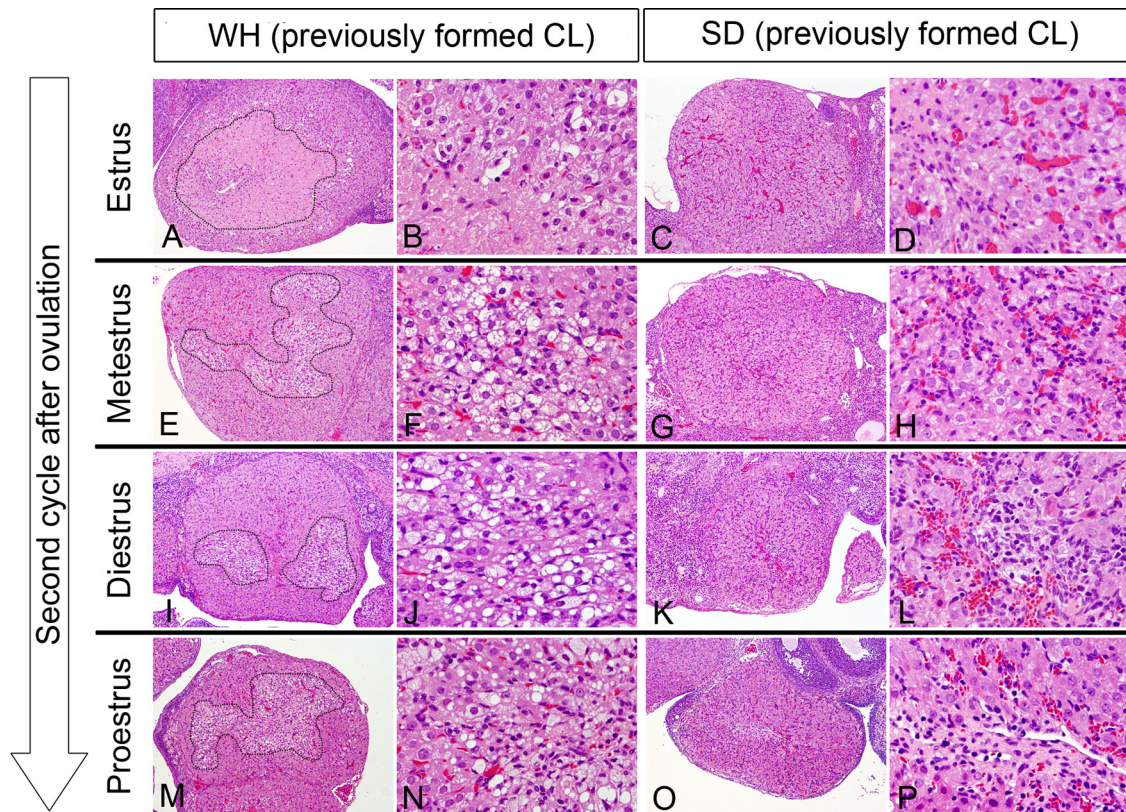


Fig. 2. Previously formed CLs in each estrous cycle at the second cycle after ovulation of WH and SD rats. After estrus, the necrotic area of the CL was replaced by foamy macrophages in WH rats (E, F, I, J, M, N), and the fibrotic area increased and interstitial cells became prominent in SD rats (G, H, K, L, O, P). Circles show the necrotic area in WH rats. HE staining. A, C, E, G, I, K, M, O; $\times 40$. B, D, F, H, J, L, N, P; $\times 300$.

proximately 1.2 times heavier than those of SD rats. These findings are consistent with a previous report⁶, suggesting that the low rate of luteolysis in WH rats maintains the size of the CL during certain estrous cycles and results in heavier ovaries.

Using image analysis software, we determined that diestrus ovaries in SD rats were smaller than those of WH rats. We assume that the reason for this difference is that the total size of the previously formed CLs has the most influ-

ence on the ovarian size rather than the currently formed CLs size, as in diestrus, and the number of large follicles is reduced to a greater extent than in other cycles¹⁰.

A previous study reported that litter sizes in WH rats acquired from a different breeder (Tac: Glx:WifBR) from that used here were smaller than those commonly reported for SD rats⁹. Further, that same study reported higher incidences of pre- and postimplantation loss and resorption than typically seen in SD rats. However, the number of ovula-

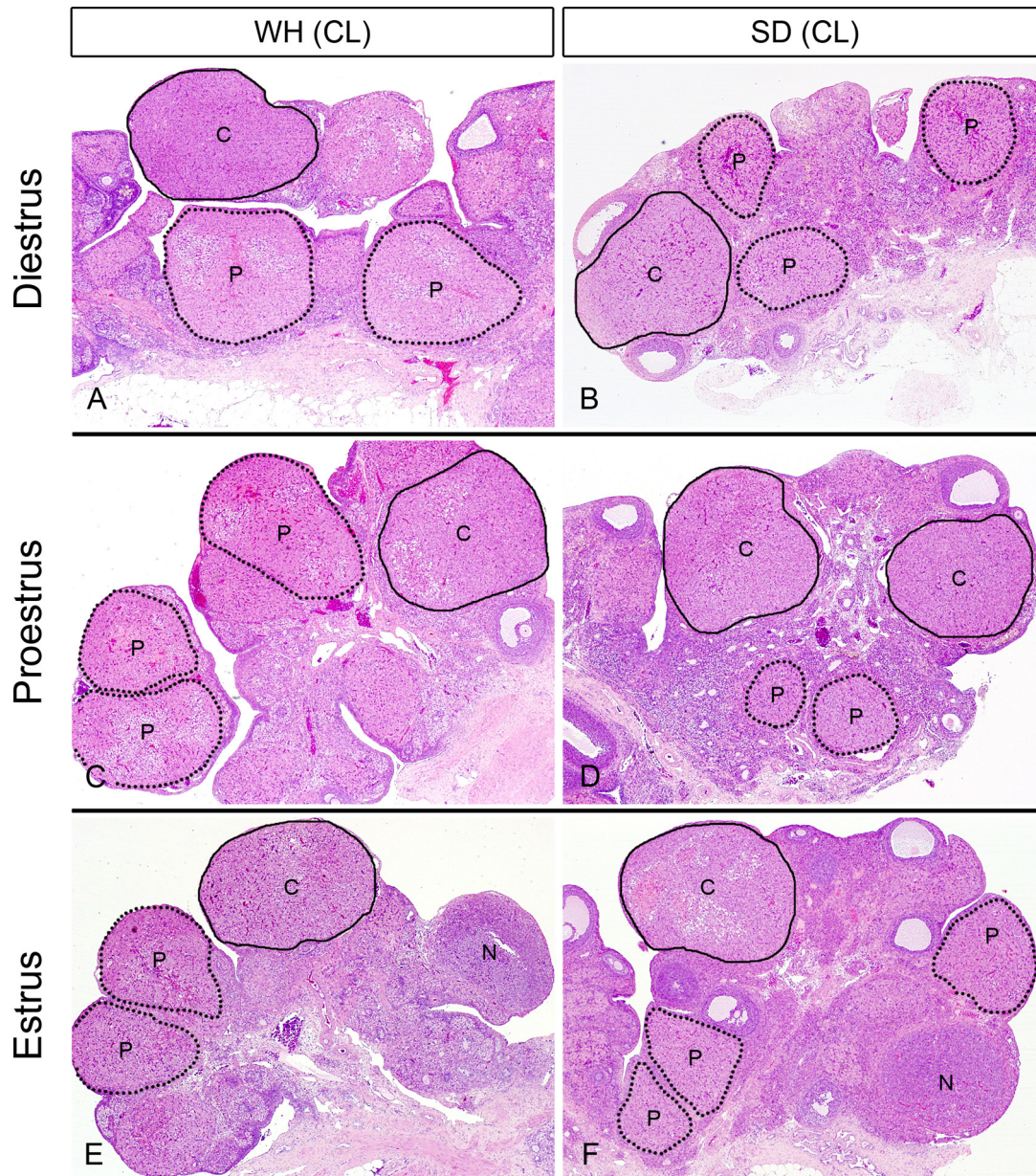


Fig. 3. Currently formed CLs and previously formed CLs in diestrus, proestrus and estrus of WH and SD rats. C=currenty formed CL, P=previously formed CL and N=newly formed CL. The sizes of the currently formed CLs were almost comparable in both strains. Previously formed CLs in SD rats were smaller than in WH rats. In each estrus, the sizes of the previously formed CLs were obviously smaller than those of the currently formed CLs in SD rats; however, the sizes of previously formed CLs of WH rats in diestrus or proestrus were considered to be the same or a little smaller compared with currently formed CLs (A and C), and smaller compared with currently formed CLs in estrus (E). HE staining. $\times 20$.

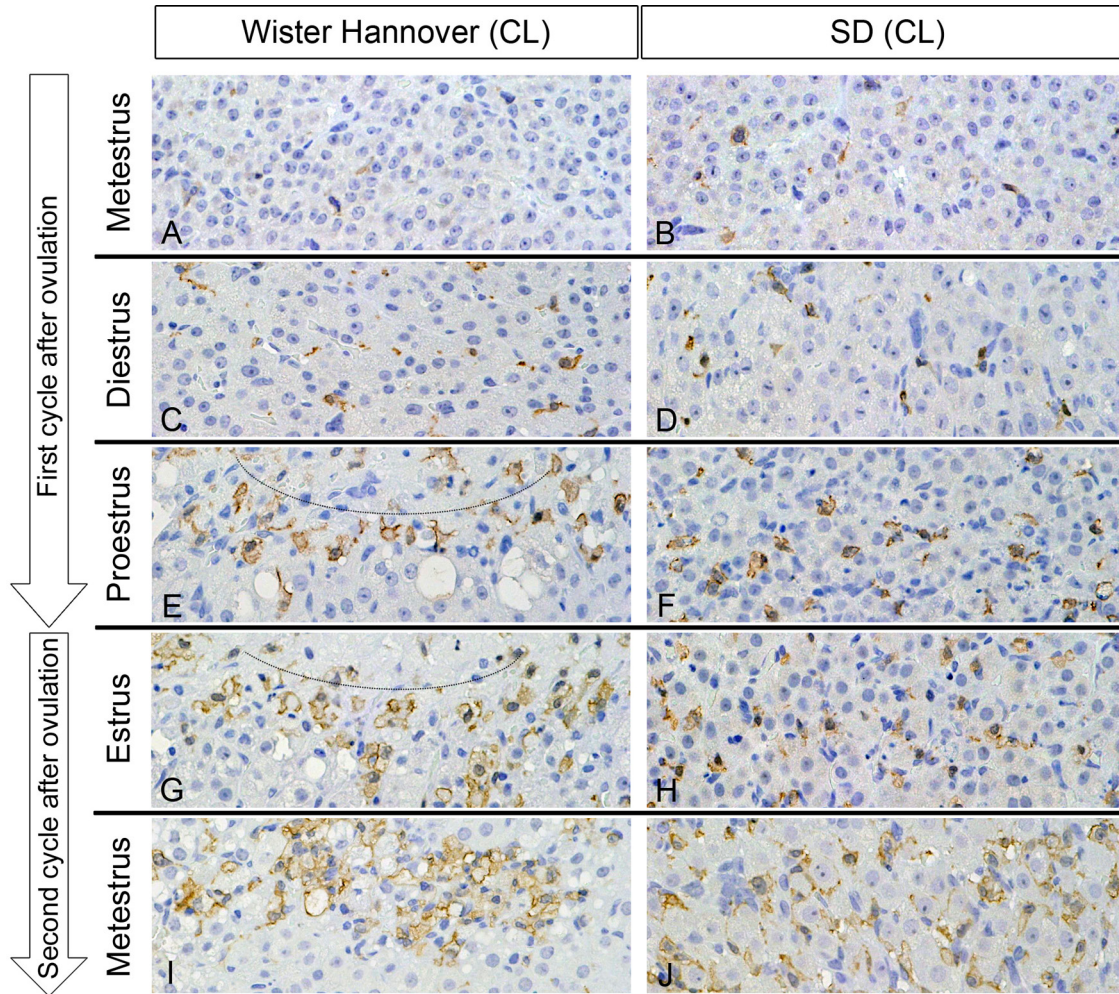


Fig. 4. Currently and previously formed CLs in WH and SD rats. The Iba-1-positive macrophages accumulated around the necrotic area (circles) in WH rats (E, G), and were widely scattered in SD rats (F, H, J) after diestrus in the first cycle after ovulation. In metestrus at the second cycle after ovulation, macrophages accumulated and replaced the necrotic area in WH rats (I). Macrophages of the CLs in metestrus and diestrus at the first cycle after ovulation were almost the same in WH (A, C) and SD (B, D) rats. Anti-Iba-1 immunostain, counterstained with hematoxylin. $\times 400$.

Table 3. Summary of Luteal Regression in WH and SD Rats

Estrous cycle	Strain	
	WH	SD
First cycle after ovulation		
Estrus	newly formed CL	newly formed CL
Metestrus	start of CL cell necrosis (massive)	start of CL cell necrosis (scattered)
Diestrus		
Proestrus		
Second cycle after ovulation		
Estrus	reduction in size of CL	reduction in size of CL
Metestrus		
Diestrus		
Proestrus		
Proestrus		

tions from bilateral ovaries was considered similar to that of SD rats, as the number of currently formed CLs was similar to that of SD rats in our investigation. These data suggest that the relatively low number of litters seen in WH rats is not caused by a reduced number of ovulations.

Prolactin (PRL) is the essential luteotropic and luteolytic hormone in the rat ovary and induces apoptosis of luteal cells (luteolysis), stimulates the proliferation of vascular cells, and regulates the number of macrophages in CLs¹¹⁻¹³. Further, WH rats exhibit a low incidence of mammary tumors compared with other strains of rats⁷. PRL is also an important hormone controlling rodent mammary gland growth¹⁴. Although hormone levels were not determined here, PRL levels likely influence the pattern and rate of CL regression and may explain the differences between each strain. In general, the preovulatory PRL surge

at proestrus induces luteal cell apoptosis by activating the Fas pathway^{15, 16}. Whereas, the typically pattern of luteolysis in WH rats was coagulative necrosis in the center of CL. Coagulative necrosis is so-called “ischemic necrosis” generally caused by infarct or decline of the bloodstream. In a previous report, PRL treatment increased the number of vascular cells in cycling rats, and dopaminergic agonist CB154 treatment decreased the number of vascular cells in pregnant rats¹¹. We speculate that the difference in vascular proliferation or distribution in newly formed CLs with or without a low PRL level may be related to the difference in the necrotic pattern of luteal cells during luteal regression between WH and SD rats. Further investigation is required to determine relevant hormone levels for the two strains.

In toxicological studies, an increased number or hypertrophy of CLs can be induced by some exogenous drugs or chemicals that affect gonadal hormone secretion, such as ethylene glycol monomethyl ether, atrazine and bromocriptine^{5, 17, 18}, via inhibition of luteolysis with or without prolactin dependence. Given that these chemicals cause different morphological changes in the CL, background data that characterize luteal regression depending on rat strain and age are required for toxicologic pathologists to accurately assess luteal toxicity in rat ovaries.

References

1. Yoshida M, Sanbuissyo A, Hisada S, Takahashi M, Ohno Y, and Nishikawa A. Morphological characterization of the ovary under normal cycling in rats and its viewpoints of ovarian toxicity detection. *J Toxicol Sci.* **34**(Suppl 1): SP189–SP197. 2009. [[Medline](#)] [[CrossRef](#)]
2. Yuan Y, and Foley GL. Female reproductive system. In: *Handbook of Toxicologic Pathology*, 2nd ed., Vol.2. WM Haschek, CG Rousseaux, MA Walling (eds). Academic Press, London. 847–894. 2002.
3. Westwood FR. The female rat reproductive cycle: a practical histological guide to staging. *Toxicol Pathol.* **36**: 375–384. 2008. [[Medline](#)] [[CrossRef](#)]
4. Imai M, Sasamoto S, and Suzuki T. Histological studies on adult mice ovaries at various stages of the estrus cycle. *Jap J Animal Reprod.* **13**: 97–102. 1967. [[CrossRef](#)]
5. Taketa Y, Inomata A, Hosokawa S, Sonoda J, Hayakawa K, Nakano K, Momozawa Y, Yamate J, Yoshida M, Aoki T, and Tsukidate K. Histopathological characteristics of luteal hypertrophy induced by ethylene glycol monomethyl ether with a comparison to normal luteal morphology in rats. *Toxicol Pathol.* **39**: 372–380. 2011. [[Medline](#)] [[CrossRef](#)]
6. Okamura T, Suzuki S, Ogawa T, Kobayashi J, Kusuoka O, Hatayama K, Mochizuki M, Hoshiya T, Okazaki S, and Tamura K. Background data for general toxicology parameters in RccHanTM: WIST rats at 8, 10, 19, and 32 weeks of age. *J Toxicol Pathol.* **24**: 195–205. 2011. [[Medline](#)] [[CrossRef](#)]
7. Weber K, Razinger T, Hardisty JF, Mann P, Martel KC, Frische EA, Blumbach K, Hillen S, Song S, Anzai T, and Chevalier HJ. Differences in rat models used in routine toxicity studies. *Int J Toxicol.* **30**: 162–173. 2011. [[Medline](#)] [[CrossRef](#)]
8. Yamatoya H, Kawaguchi H, Yajima K, Kadokura H, Yoshikawa T, Yamashita R, Shiraishi M, Miyamoto A, and Miyoshi N. Data on Wistar Hannover rats from a general toxicity study. *Exp Anim.* **61**: 467–476. 2012. [[Medline](#)] [[CrossRef](#)]
9. Liberati TA, Roe BJ, and Feuston MH. An oral (gavage) control embryo-fetal development study in the Wistar Hannover rat. *Drug Chem Toxicol.* **25**: 109–130. 2002. [[Medline](#)] [[CrossRef](#)]
10. Mandl AM, and Zuckerman S. Cyclical changes in the number of medium and large follicles in the adult rat ovary. *J Endocrinol.* **8**: 341–346. 1952. [[Medline](#)] [[CrossRef](#)]
11. Gaytan F, Morales C, Bellido C, Aguilar E, and Sanchez-Criado JE. Role of prolactin in the regulation of macrophages and in the proliferative activity of vascular cells in newly formed and regressing rat corpora lutea. *Biol Reprod.* **57**: 478–486. 1997. [[Medline](#)] [[CrossRef](#)]
12. Bowen JM, Towns R, Warren JS, and Landis Keyes P. Luteal regression in the normally cycling rat: apoptosis, monocyte chemoattractant protein-1, and inflammatory cell involvement. *Biol Reprod.* **60**: 740–746. 1999. [[Medline](#)] [[CrossRef](#)]
13. Gaytán F, Bellido C, Morales C, and Sánchez-Criado JE. Luteolytic effect of prolactin is dependent on the degree of differentiation of luteal cells in the rat. *Biol Reprod.* **65**: 433–441. 2001. [[Medline](#)] [[CrossRef](#)]
14. Rudmann D, Cardiff R, Chouinard L, Goodman D, Küttler K, Marxfeld H, Molinolo A, Treumann S, and Yoshizawa K. INHAND Mammary, Zymbal’s, Preputial, and Clitoral Gland Organ Working Group. Proliferative and nonproliferative lesions of the rat and mouse mammary, Zymbal’s, preputial, and clitoral glands. *Toxicol Pathol.* **40**(Suppl): 7S–39S. 2012. [[Medline](#)] [[CrossRef](#)]
15. Kuranaga E, Kanuka H, Bannai M, Suzuki M, Nishihara M, and Takahashi M. Fas/Fas ligand system in prolactin-induced apoptosis in rat corpus luteum: possible role of luteal immune cells. *Biochem Biophys Res Commun.* **260**: 167–173. 1999. [[Medline](#)] [[CrossRef](#)]
16. Sugino N, and Okuda K. Species-related differences in the mechanism of apoptosis during structural luteolysis. *J Reprod Dev.* **53**: 977–986. 2007. [[Medline](#)] [[CrossRef](#)]
17. Sanbuissho A, Yoshida M, Hisada S, Sagami F, Kudo S, Kumazawa T, Ube M, Komatsu S, and Ohno Y. Collaborative work on evaluation of ovarian toxicity by repeated-dose and fertility studies in female rats. *J Toxicol Sci.* **34**(Suppl 1): SP1–SP22. 2009. [[Medline](#)] [[CrossRef](#)]
18. Taketa Y, Inoue K, Takahashi M, Yamate J, and Yoshida M. Differential morphological effects in rat corpora lutea among ethylene glycol monomethyl ether, atrazine, and bromocriptine. *Toxicol Pathol.* **41**: 736–743. 2013. [[Medline](#)] [[CrossRef](#)]